ELSEVIER

Journal of Organometallic Chemistry 623 (2001) 153–160

Journal of Organometallic Chemistry

www.elsevier.nl/locate/jorganchem

Hypervalent tellurium compounds containing N → Te intramolecular interactions. Crystal and molecular structure of $[2\text{-}(Me_2NCH_2)C_6H_4]_2Te_2$, $[2\text{-}(Me_2NCH_2)C_6H_4]TeS(S)PR_2$ (R = Me, Ph, OPr^i) and $[2\text{-}(Me_2NCH_2)C_6H_4]Te–S–PPh_2{=}N–PPh_2{=}S$

John E. Drake* [a,1], Michael B. Hursthouse [b], Monika Kulcsar [c], Mark E. Light [b], Anca Silvestru* [c,2]

[a] *Department of Chemistry and Biochemistry, University of Windsor, Windsor, Ont., Canada, N9B 3P4*
[b] *Department of Chemistry, University of Southampton, Highfield, Southampton SO17 1BJ, UK*
[c] *Chemistry Department, 'Babes-Bolyai' University, RO-3400 Cluj-Napoca, Romania*

Received 10 August 2000

Abstract

$[2\text{-}(Me_2NCH_2)C_6H_4]TeS(S)PR_2$ [R = Me (**2**), Et (**3**), Ph (**4**), OPr^i (**5**)] were prepared by reacting $[2\text{-}(Me_2NCH_2)C_6H_4]_2Te_2$ (**1**) with the appropriate disulfanes, $[R_2P(S)S]_2$, while $[2\text{-}(Me_2NCH_2)C_6H_4]Te–S–PPh_2{=}N–PPh_2{=}S$ (**6**) was obtained by metathesis reaction between $[2\text{-}(Me_2NCH_2)C_6H_4]TeBr$ and potassium tetraphenyldithioimidodiphosphinate. The compounds were characterized by multinuclear NMR (^1H, ^{13}C, ^{31}P). The crystal and molecular structures of **1**, **2**, **4**–**6** were determined by single-crystal X-ray diffraction. All compounds are monomeric and the N atom of the pendant CH_2NMe_2 arm is strongly coordinated to the tellurium atom. The organophosphorus ligands are monodentate, thus resulting in a T-shaped coordination geometry around tellurium.

1. Introduction

The chemistry of organotellurium compounds containing intramolecular N → Te interactions has received considerable interest in recent years due to the enhanced thermal and hydrolytic stability of these compounds [1–8]. Several derivatives containing *ortho*-tellurated benzylamino moieties have been reported [4–6,8–11] and a general feature was found to be the intramolecular coordination of the nitrogen atom of the pendant arm to the tellurium atom. In order to investigate the effect on the N → Te interaction of the ligand *trans* to nitrogen, we decided to use dithio ligands. A few organotellurium compounds containing both (*C*,*N*) and dithiocarbamato ligands have been reported so far, i.e. $RTeS(S)CNR'_2$ [R′ = Me, R = 2-phenylazophenyl [12], 2-(2-pyridyl)phenyl [13], 2-(2-quinolinyl)phenyl [14]; R′ = Et, R = 2-(dimethylaminomethyl)phenyl [8]] and $RTe[S(S)CNEt_2]_3$ [R = 2-(dimethylaminomethyl)phenyl [8], 2-{1-(dimethylamino)ethyl}phenyl [9]], but no derivatives containing thiophosphorus ligands are described [15]. On the other hand, dithiophosphinato ligands, $[R_2P(S)S]^-$ [16–20], as well as tetraorganodichalcogenoimidodiphosphinato ligands, $[(XPR_2)(YPR'_2)N]^-$ [20–27], are well known usually to involve both chalcogen atoms in coordination to the tellurium atom, resulting in either chelate (a) or bridging (b) structures:

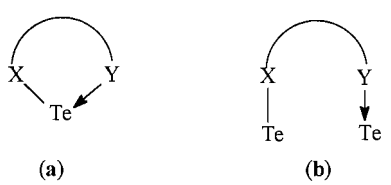

(a) (b)

Here we report on the synthesis and spectroscopic characterization of some complexes derived from *ortho*-tellurated (dimethylaminomethyl)benzene which con-

[1] *Corresponding author. Fax: +1-519-9737098.
[2] *Also corresponding author.

0022-328X/01/$ - see front matter
PII: S0022-328X(00)00739-7

tain dithiophosphorus ligands, as well as the crystal and molecular structures of $[2\text{-}(Me_2NCH_2)C_6H_4Te]_2$, $[2\text{-}(Me_2NCH_2)C_6H_4]TeS(S)PR_2$ [R = Me, Ph, OPr^i] and $[2\text{-}(Me_2NCH_2)C_6H_4]Te–S–PPh_2=N–PPh_2=S$.

2. Results and discussion

2.1. Preparation

The diorganodithiophosphinato (**2**–**4**) and diisopropyldithiophosphato (**5**) derivatives were obtained according to Eq. (1), by reacting stoichiometric amounts of the diorganoditelluride, $[2\text{-}(Me_2NCH_2)C_6H_4Te]_2$, and the corresponding bis(diorganothiophosphinyl)disulfane, $[R_2P(S)S]_2$ (R = Me, Et, Ph, OPr^i), at room temperature, in methylene chloride:

$$[2\text{-}(Me_2NCH_2)C_6H_4Te]_2 + [R_2P(S)S]_2 \rightarrow \underset{\mathbf{1}}{} 2\ [2\text{-}(Me_2NCH_2)C_6H_4]TeS(S)PR_2$$

R = Me (**2**), Et (**3**), Ph (**4**), OPr^i (**5**) (1)

The tetraphenyldithioimidodiphosphinato analog (**6**) was prepared by refluxing stoichiometric amounts of organotellurium(II) bromide and $K[(SPPh_2)_2N]$, in acetone, according to Eq. (2)

$$[2\text{-}(Me_2NCH_2)C_6H_4]TeBr + K[(SPPh_2)_2N] \rightarrow$$

$$\underset{\mathbf{6}}{[2\text{-}(Me_2NCH_2)C_6H_4]Te–S–PPh_2=N–PPh_2=S} + KBr \quad (2)$$

The resulting compounds are yellow, crystalline solids, which can be recrystallized from chloroform or methylene chloride. All compounds were characterized by multinuclear NMR spectroscopy (^1H, ^{13}C and ^{31}P) and the crystal and molecular structures of compounds **1**, **2**, **4**–**6** have been determined by single-crystal X-ray diffraction.

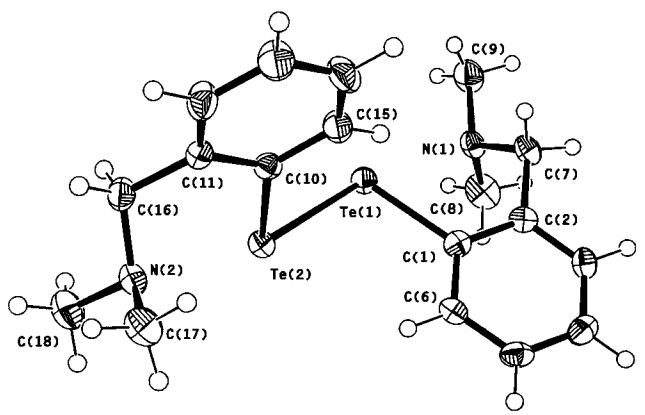

Fig. 1. ORTEP plot of the molecule $[2\text{-}(Me_2NCH_2)C_6H_4]_2Te_2$ (**1**). The atoms are drawn with 40% probability ellipsoids except for the hydrogen atoms.

2.2. NMR spectra and structure

The ^1H and ^{13}C chemical shifts for all tellurium(II) compounds investigated in this work exhibit a trend that is indicative of *ortho* telluration and N → Te coordination. Thus, both NMe_2 (δ 2.5–2.6 ppm) and methylene (δ 3.7–3.8 ppm) resonances (^1H-NMR) are shifted downfield in the $[2\text{-}(Me_2NCH_2)C_6H_4]TeS(S)PR_2$ derivatives with respect to the free dimethylbenzylamine (cf. $PhCH_2NMe_2$ [8]: δ 2.25 and 3.43 ppm, respectively). However, this effect is less pronounced in the case of $[2\text{-}(Me_2NCH_2)C_6H_4]Te[(SPPh_2)_2N]$ (δ 2.34 and 3.49 ppm, respectively). The singlet pattern of the NMe_2 and CH_2 resonances of the $[2\text{-}(Me_2NCH_2)C_6H_4]Te–$ moiety in the ^1H-NMR spectra suggests the equivalence in solution of the methyl and methylene protons at room temperature on the NMR timescale. The assignment of the carbon resonances according to the numbering scheme (c) was made using the spectra of the starting materials and literature data (resonances for C_1 and C_2 were not observed) [4,8]. The telluration of the skeleton in position 1 is reflected in a downfield shift of ca. 10 ppm of the C_6 resonances (δ 134.01 for **3**, and 134.46 for **4**, versus 127.6 ppm for free $PhCH_2NMe_2$) [8].

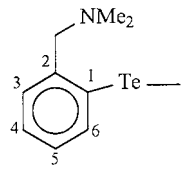

(c)

As expected, the proton and carbon resonances corresponding to the organic groups attached to phosphorus are split into two components of equal intensity, due to phosphorus–proton and phosphorus–carbon coupling, respectively. The methyl protons of the isopropyl groups in **5** are not equivalent, two doublet signals being observed in the ^1H-NMR spectrum.

The ^{31}P-NMR spectra of the dithiophosphinato and dithiophosphato derivatives exhibit one singlet resonance. By contrast, for the tetraphenyldithioimidodiphosphinato compound **6** two singlet ^{31}P resonances are observed, a behavior consistent with a monodentate coordination of the ligand to the tellurium atom.

2.3. Crystal and molecular structure of $[2\text{-}(Me_2NCH_2)C_6H_4Te]_2$ (**1**)

The molecular structure of **1** with the atom numbering scheme is shown in Fig. 1 and selected interatomic distances and angles are listed in Table 1. The crystal of **1** consists of monomeric molecules which exhibit a

Table 1
Important interatomic distances (Å) and angles (°) for [2-$(Me_2NCH_2)C_6H_4Te]_2$ (**1**)

Te(1)–Te(2)	2.7493(6)		
Te(1)–C(1)	2.143(4)	Te(2)–C(10)	2.132(4)
N(1)–C(7)	1.459(5)	N(2)–C(16)	1.462(5)
N(1)–C(8)	1.460(5)	N(2)–C(17)	1.448(6)
N(1)–C(9)	1.463(5)	N(2)–C(18)	1.462(5)
C(1)–Te(1)–Te(2)	99.51(12)	C(10)–Te(2)–Te(1)	98.42(12)
C(7)–N(1)–C(8)	111.7(3)	C(16)–N(2)–C(17)	111.8(3)
C(7)–N(1)–C(9)	110.7(3)	C(16)–N(2)–C(18)	110.9(3)
C(8)–N(1)–C(9)	110.5(4)	C(17)–N(2)–C(18)	110.2(4)
N(1)–C(7)–C(2)	110.9(3)	N(2)–C(16)–C(11)	111.0(3)

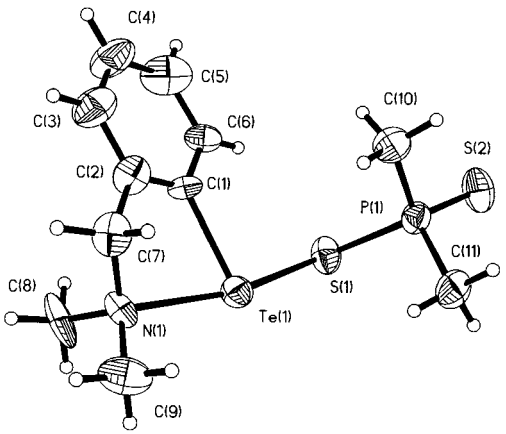

Fig. 2. ORTEP plot of the molecule [2-$(Me_2NCH_2)C_6H_4$]TeS(S)PMe_2 (**2**). The atoms are drawn with 50% probability ellipsoids.

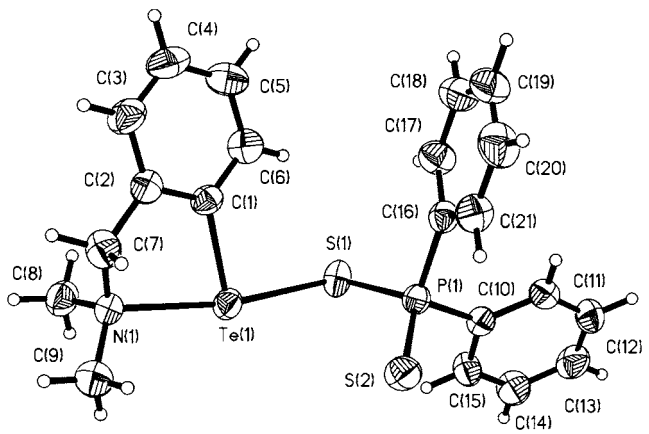

Fig. 3. ORTEP plot of the molecule [2-$(Me_2NCH_2)C_6H_4$]TeS(S)PPh_2 (**4**). The atoms are drawn with 50% probability ellipsoids.

T-shaped geometry around both tellurium atoms as a result of the intramolecular N→Te interactions. The tellurium–nitrogen interatomic distances [N(1)···Te(1) 2.84 Å, N(2)···Te(2) 2.90 Å] are much shorter than the sum of the van der Waals radii for tellurium and nitrogen (3.65 Å) [28] and comparable with those observed in the tellurane [2-$(Me_2NCH_2)C_6H_4]_2$Te (3.048, 3.145 Å) [4]. These Te–N distances are however considerably longer than those observed in the organophosphorus derivatives described below, thus reflecting the lower electronegativity of X placed in the *trans* position relative to N in the X–Te···N fragment. The cordination geometry around the Te atoms can be described as *pseudo*-trigonal bipyramidal, with N and the second Te atoms in axial positions [N(1)···Te(1)–Te(2) 169.4°, N(2)···Te(2)–Te(1) 166.2°] and two lone pairs and the carbon atom in the equatorial plane.

The Te–Te distance in **1** [2.7493(6) Å] is somewhat longer than those observed in other R_2Te_2 derivatives [2.712(2) Å in Ph_2Te_2 [29], and 2.697(3) Å in *p*-Tol_2Te_2 [30], respectively] or in $Te_2(S_2PPh_2)_2$ [2.723(1) Å] [16], probably due to the *trans* effect of the Te···N interactions.

The five-membered TeC_3N rings are not planar, but folded along the Te(1)···C(7) and Te(2)···C(16) axes, respectively, with the nitrogen atoms −0.943 and −0.979 Å out of the plane of the rest of the atoms. The two rings are twisted, one relative to the other, with a dihedral angle of 99.5° between best Te(1)/C(1)/C(2)/C(7) and Te(2)/C(10)/C(11)/C(16) planes.

2.4. Crystal and molecular structure of [2-$(Me_2NCH_2)C_6H_4$]TeS(S)PR_2 [R = Me (**2**), Ph (**4**), OPr^i (**5**)]

The molecular structures of **2**, **4** and **5** with the atom numbering scheme are shown in Figs. 2–4, respectively, and selected interatomic distances and angles are listed in Table 2. All three compounds exhibit similar monomeric structures and no intermolecular interactions have been observed.

The compounds are almost T-shaped as a result of the N→Te intramolecular interactions. The tellurium–nitrogen distances [2.469(12) Å in **2**, 2.439(2) Å in **4** and 2.467(3) Å in **5**, respectively] are shorter than in **1**

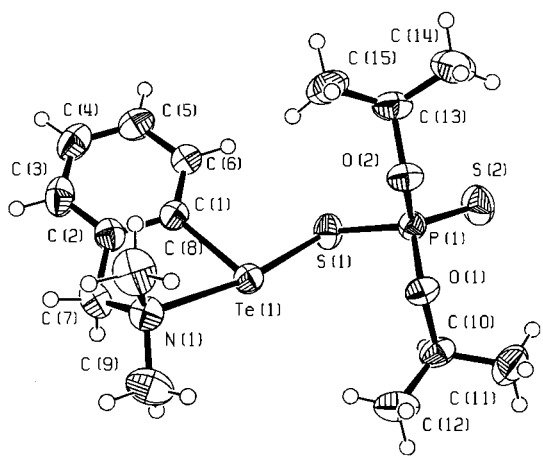

Fig. 4. ORTEP plot of the molecule [2-$(Me_2NCH_2)C_6H_4$]TeS(S)-$P(OPr^i)_2$ (**5**). The atoms are drawn with 50% probability ellipsoids.

Table 2
Important interatomic distances (Å) and angles (°) for [2-(Me_2NCH_2)C_6H_4]TeS(S)PR_2 derivatives [R = Me (**2**), Ph (**4**), OPr^i (**5**)]

	2	**4**	**5**
Te(1)–C(1)	2.16(2)	2.126(3)	2.118(3)
Te(1)–N(1)	2.48(2)	2.439(2)	2.467(3)
Te(1)–S(1)	2.526(6)	2.5416(11)	2.5388(16)
S(1)–P(1)	2.076(8)	2.0795(12)	2.0397(13)
S(2)–P(1)	1.947(8)	1.9479(14)	1.9262(16)
N(1)–C(7)	1.47(3)	1.468(3)	1.474(4)
N(1)–C(8)	1.45(3)	1.474(4)	1.458(5)
N(1)–C(9)	1.46(3)	1.467(4)	1.465(5)
C(1)–Te(1)–N(1)	73.6(7)	76.04(9)	75.28(11)
C(1)–Te(1)–S(1)	95.0(6)	95.16(8)	92.13(9)
N(1)–Te(1)–S(1)	166.7(4)	169.86(6)	167.03(7)
P(1)–S(1)–Te(1)	107.1(3)	105.88(5)	101.78(5)
S(2)–P(1)–S(1)	109.5(4)	117.09(6)	108.19(6)
C(9)–N(1)–C(7)	111(2)	112.4(3)	111.4(3)
C(9)–N(1)–C(8)	112(2)	110.0(2)	111.5(3)
C(7)–N(1)–C(8)	111(2)	110.5(2)	111.2(3)
C(9)–N(1)–Te(1)	111(2)	110.1(2)	109.9(2)
C(7)–N(1)–Te(1)	101.4(12)	104.4(2)	101.4(2)
C(8)–N(1)–Te(1)	109.5(13)	109.3(2)	110.9(2)

(average N–Te 2.87 Å), consistent with the higher electronegativity of the S atom placed in the *trans* position relative to N(1) in the X–Te–N fragment. However, the intramolecular N–Te distances in these organophosphorus derivatives are longer than the values reported for related dithiocarbamato derivatives, $RTeS(S)CNMe_2$, i.e. 2.340 Å (R = 2-phenylazophenyl) [12], 2.354 Å [2-(2-pyridyl)phenyl] [13], average 2.375 Å [2-(2-quinolinyl)phenyl] [14]. The overall coordination about the tellurium atoms can be considered as essentially *pseudo*-trigonal bipyramidal, with C(1) and lone pairs in the equatorial positions and N(1) and S(1) atoms in axial ones [N(1)–Te(1)–S(1) 166.7(4)° in **2**, 169.86(6)° in **4** and 167.03(7)° in **5**]. The distortion of the coordination geometry is mainly due to constraints arising from the five-membered chelate rings, particularly the N(1)–Te(1)–C(1) angle [73.6(7)° in **2**, 76.04(9)° in **4** and 75.28(11)° in **5**, respectively]. The five-membered TeC_3N rings are again non-planar, i.e. folded along the Te(1)···$C_{methylene}$ axis, with the N(1) atoms 0.803 Å in **2**, −0.627 Å in **4** and −0.762 Å in **5**, respectively, out of the best Te(1)/C(1)/C(2)/C(7) plane.

The dithio ligands act in all cases as monodentate moieties, only one sulfur atom being connected to the tellurium atom. The Te(1)–S(1) bond distances [2.526(6) Å in **2**, 2.5416(11) Å in **4** and 2.5388(16) Å in **5**] are within the expected range for covalent tellurium–sulfur single bonds [15]. However, they are significantly longer than the value of 2.406(2) Å observed in $PhTeS(S)PPh_2$ [18], where a polymeric zig-zag chain is built through bridging Ph_2PS_2 units, i.e. single Te(1)–S(–P) bonds and weak Te(2)···S(=P) [3.989(2) Å] secondary interactions.

In all title [2-(Me_2NCH_2)C_6H_4]TeS(S)PR_2 derivatives, the second sulfur atom of the 1,1-dithiophosphorus ligands is not involved in any intra- or intermolecular interaction to tellurium atoms. This behavior is also reflected in the magnitude of the phosphorus–sulfur distances within the ligand moiety, which are consistent with single P–S and double P=S bonds [e.g. P(1)–S(1) 2.0795(12) Å, P(1)–S(2) 1.9479(14) Å in **4**, versus P–S 2.077(1) Å and P=S 1.954(1) Å in $Ph_2P(S)SH$ [31]]. However, the relative position of the sulfur atom double bonded to phosphorus with respect to the tellurium atom is different. Thus in **2** and **5** the non-bonded sulfur atom is twisted as far as possible from the tellurium atom [intramolecular non-bonding Te(1)···S(2) distances are 5.487 Å in **2** and 5.336 Å in **5**]. By contrast, in **4** the 1,1-dithio ligand moiety is twisted to bring the non-bonded S(2) atom much closer to the tellurium atom [Te(1)···S(2) 3.878 Å]. This close intramolecular Te(1)···S(2) contact might suggest a weak interaction as observed in some related dimethyldithiocarbamato derivatives, $RTeS(S)CNMe_2$, i.e. 3.225(3) Å (R = 2-phenylazophenyl) [12], average 3.226(1) Å [2-(2-quinolinyl)phenyl] [14], or 3.667 Å [2-(2-pyridyl)phenyl] [13]. Probably, this behavior is due to packing forces in the crystal, since no such intramolecular interaction was observed in **6**, which contains a much more flexible ligand.

2.5. Crystal and molecular structure of [2-(Me_2NCH_2)C_6H_4]Te–S–PPh_2=N–PPh_2=S (**6**)

The molecular structure of **6** with the atom numbering scheme is shown in Fig. 5 and selected interatomic distances and angles are listed in Table 3. The crystal of **6** consists of monomeric molecules which also exhibit a T-shaped geometry around the tellurium atom as result of the intramolecular N→Te interaction [N(1)–Te(1) 2.430(3) Å, N(1)–Te(1)–S(1) 166.11(7)°]. The five-membered TeC_3N ring is again folded along the Te(1)···$C_{methylene}$ axis, with the N(1) atom 0.786 Å out from the best Te(1)/C(1)/C(2)/C(7) plane.

The tetraphenyldithioimidodiphosphinato ligand is well known for its ability to act as a bidentate moiety, i.e. both sulfur atoms being involved in coordination to a tellurium(II) center, thus leading to chelate or bridging structures [21,22,25,26]. Surprisingly, in **6** the dithio ligand moiety is monodentate, only the S(1) atom being connected to Te(1) [Te–S(1) 2.5504(11) Å]. The second sulfur atom is involved neither in intramolecular [nonbonding Te(1)···S(2) 5.502 Å] nor in intermolecular interactions to a tellurium atom. This contrasts with the dimeric structure of $RTe[(SPPh_2)_2N]$ (R = Ph [22], 4-$MeOC_6H_4$ [25]) built through bridging dithioimidodiphosphinato ligands (cf. $PhTe[(SPPh_2)_2N]$ [22]:

Te(1)–S(1) 2.557(3), Te(2)–S(2) 2.843(3) Å]. The unusual behavior of this particular ligand in **6** is also reflected in different phosphorus–sulfur and phosphorus–nitrogen distances within the highly flexible SPNPS skeleton, which correspond to single [P(1)–S(1) 2.0568(13), P(2)–N(2) 1.612(3) Å] and double [P(2)–S(2) 1.9449(14), P(1)–N(2) 1.557(3) Å] bonds, respectively (cf. PhTe[$(SPPh_2)_2N$] [22]: P(1)–S(1) 2.044(4), P(1)–N(1) 1.580(7), P(2)–N(1) 1.589(7), P(2)–S(2) 1.996(3) Å; Me_3Sn–S–PPh_2=N–PPh_2=S [32]: P(1)–S(1) 2.048(3), P(1)–N(1) 1.572(5), P(2)–N(1) 1.605(5), P(2)–S(2) 1.972(3) Å].

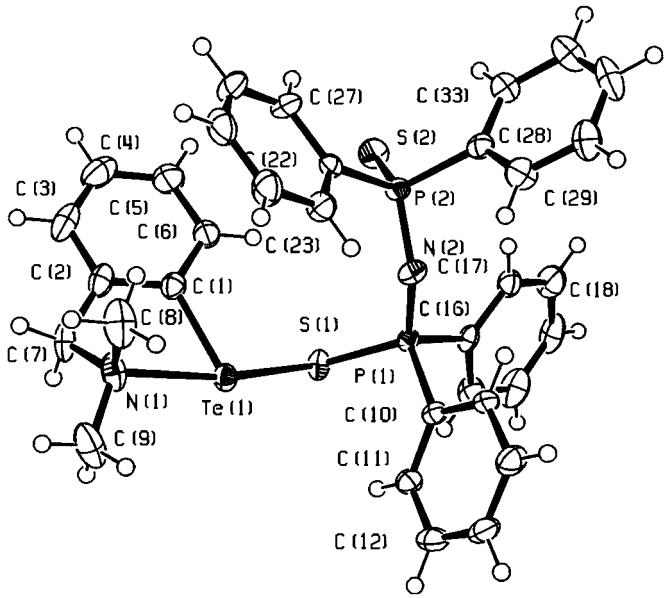

Fig. 5. ORTEP plot of the molecule [2-$(Me_2NCH_2)C_6H_4$]Te–S–PPh_2=N–PPh_2=S (**6**). The atoms are drawn with 50% probability ellipsoids.

Table 3
Important interatomic distances (Å) and angles (°) for [2-$(Me_2NCH_2)C_6H_4$]Te[$(SPPh_2)_2N$] (**6**)

Te(1)–C(1)	2.120(3)	S(1)–P(1)	2.0568(13)
Te(1)–N(1)	2.430(3)	S(2)–P(2)	1.9449(14)
Te(1)–S(1)	2.5504(11)	P(1)–N(2)	1.557(3)
N(1)–C(8)	1.473(6)	P(2)–N(2)	1.612(3)
N(1)–C(9)	1.465(6)		
N(1)–C(7)	1.471(5)		
C(1)–Te(1)–N(1)	74.98(13)	P(1)–S(1)–Te(1)	103.56(4)
C(1)–Te(1)–S(1)	92.19(10)	N(2)–P(1)–S(1)	120.67(12)
N(1)–Te(1)–S(1)	166.11(7)	P(1)–N(2)–P(2)	137.8(2)
		N(2)–P(2)–S(2)	121.65(12)
C(9)–N(1)–C(7)	111.0(3)	C(7)–N(1)–Te(1)	101.9(2)
C(7)–N(1)–C(8)	111.8(3)	C(9)–N(1)–Te(1)	110.1(3)
C(9)–N(1)–C(8)	110.1(4)	C(8)–N(1)–Te(1)	111.8(2)

3. Experimental

3.1. Materials and procedures

All manipulations were carried out under vacuum or argon by Schlenk techniques. Solvents were dried and distilled prior to use. The starting materials were prepared according to literature methods: [2-$(Me_2NCH_2)C_6H_4Te]_2$ [4], [2-$(Me_2NCH_2)C_6H_4$]TeBr [8], $[R_2P(S)S]_2$ (R = Me [33], Et [34], Ph [35], OPr^i [36],), K[$(SPPh_2)_2N$] [37]. The ^{1}H-, ^{13}C- and ^{31}P-NMR spectra were recorded on a Varian Gemini 300S instrument operating at 299.5, 75.4 and 121.4 MHz, respectively, using solutions in dried $CDCl_3$. The chemical shifts are reported in ppm relative to TMS and H_3PO_4 85%, respectively.

3.2. General procedure for the preparation of *[2-$(Me_2NCH_2)C_6H_4$]TeS(S)PR_2*

Stoichiometric amounts of [2-$(Me_2NCH_2)C_6H_4Te]_2$ and the corresponding disulfane, $[R_2P(S)S]_2$ (R = Me, Et, Ph, OPr^i), were stirred in 30 ml of methylene dichloride for 12 h at room temperature. The yellow solution was concentrated under reduced pressure to minimum volume and then kept at low temperature (−20°C) for 24 h, when the title compound deposited as a yellow cristalline solid. The solid compound was filtered off and recrystallized from methylene dichloride–*n*-hexane (1:5 by volume). Details of the preparations, melting points, yields and microanalyses (C, H, N) are given in Table 4.

[2-$(Me_2NCH_2)C_6H_4$]TeS(S)PMe_2 (**2**). ^{1}H-NMR: δ 2.09d (6H, P–CH_3, $^2J_{PH}$ = 12.8 Hz), 2.57s (6H, N–CH_3), 3.80s (2H, –CH_2–), 7.14m (3H, –C_6H_4–, H_{3-5}), 8.06d (1H, –C_6H_4–, H_6, $^3J_{HH}$ = 7.3 Hz). ^{31}P-NMR: δ 57.9s.

[2-$(Me_2NCH_2)C_6H_4$]TeS(S)PEt_2 (**3**). ^{1}H-NMR: δ 1.19dt (6H, P–CH_2–CH_3, $^3J_{HH}$ = 7.4 Hz, $^3J_{PH}$ = 20.9 Hz), 2.12dq (4H, P–CH_2–CH_3, $^3J_{HH}$ = 7.4 Hz, $^2J_{PH}$ = 7.9 Hz), 2.53s (6H, N–CH_3), 3.77s (2H, –CH_2–), 7.11m (3H, –C_6H_4–, H_{3-5}), 8.04d (1H, –C_6H_4–, H_6, $^3J_{HH}$ = 7.2 Hz). ^{13}C-NMR: δ 7.63s (P–CH_2–CH_3), 29.90d (P–CH_2–CH_3, $^1J_{PC}$ = 51.5 Hz), 45.57s (N–CH_3), 66.31s (–CH_2–), 126.98s (C_5), 127.26s (C_4), 128.67s (C_3), 134.01s (C_6). ^{31}P-NMR: δ 79.7s.

[2-$(Me_2NCH_2)C_6H_4$]TeS(S)PPh_2 (**4**). ^{1}H-NMR: δ 2.51s (6H, N–CH_3), 3.68s (2H, –CH_2–), 7.04m (3H, –C_6H_4–, H_{3-5}), 7.34m (6H, P–C_6H_5-*meta* + *para*), 7.87d (1H, –C_6H_4–, H_6, $^3J_{HH}$ = 6.9 Hz), 7.98dd (4H, P–C_6H_5-*ortho*, $^3J_{HH}$ = 6.5 Hz, $^3J_{PH}$ = 13.1 Hz). ^{13}C-NMR: δ 45.62s (N–CH_3), 66.47s (–CH_2–), 126.73s (C_5), 126.82s (C_4), 128.38d (P–C_6H_5-*meta*, $^3J_{PC}$ = 13.1 Hz), 128.50s (C_3), 130.87d (P–C_6H_5-*para*, $^4J_{PC}$ = 2.9 Hz), 131.51d (P–C_6H_5-*ortho*, $^2J_{PC}$ = 10.8 Hz), 134.46s (C_6). ^{31}P-NMR: δ 65.5s.

Table 4
Preparation and elemental analyses for $[2\text{-}(Me_2NCH_2)C_6H_4]TeS(S)PR_2$ derivatives

Starting materials		Product $[2\text{-}(Me_2NCH_2)C_6H_4]TeS(S)PR_2$ yield (g (%))	M.p. (°C)	Found (calc.) (%)		
$[2\text{-}(Me_2NCH_2)\text{-}C_6H_4]_2Te_2$ (g/mmol)	$[R_2P(S)S]_2$ (g/mmol)			C	H	N
0.33/0.63	R = Me 0.16/0.63	**2**, 0.175 (35)	144	34.28 (34.14)	4.35 (4.65)	3.74 (3.62)
0.31/0.59	R = Et 0.18/0.59	**3**, 0.1 (20)	123	37.37 (37.62)	5.12 (5.30)	3.43 (3.37)
0.17/0.32	R = Ph 0.16/0.32	**4**, 0.24 (63)	143–145	49.13 (49.35)	4.28 (4.31)	2.71 (2.74)
0.27/0.51	R = OPr^i 0.22/0.51	**5**, 0.17 (36)	82–83	37.79 (37.92)	5.44 (5.48)	3.02 (2.95)

$[2\text{-}(Me_2NCH_2)C_6H_4]TeS(S)P(OPr^i)_2$ (**5**). ^{1}H-NMR: δ 1.23d [6H, P–O–CH(CH_3)$_2$, $^3J_{HH} = 6.1$ Hz], 1.29d [6H, P–O–CH(CH_3)$_2$, $^3J_{HH} = 6.1$ Hz], 2.57s (6H, N–CH_3), 3.78s (2H, –CH_2–), 4.81dh [2H, P–O–CH(CH_3)$_2$, $^3J_{HH} = 6.1$ Hz, $^3J_{PH} = 12.4$ Hz], 7.13m (3H, –C_6H_4–, H_{3-5}), 8.07d (1H, –C_6H_4–, H_6, $^3J_{HH} = 7.4$ Hz). ^{31}P-NMR: δ 95.3s.

3.3. Preparation of *[2-(Me$_2$NCH$_2$)C$_6$H$_4$]Te–S–PPh$_2$=N–PPh$_2$=S (6)*

$[2\text{-}(Me_2NCH_2)C_6H_4]TeBr$ (0.29 g, 0.84 mmol) and $K[(SPPh_2)_2N]$ (0.30 g, 0.84 mmol) were stirred in 25 ml acetone, at reflux for 5 h. The KBr was filtered off from the reaction mixture and the yellow solution was concentrated under reduced pressure until a yellow solid deposited. The product was filtered off and was recrystallized from methylene dichloride–*n*-hexane (1:5 by volume). Yield: 0.15 g (30%). M.p. 140°C. Anal. Calc. for $C_{33}H_{32}N_2P_2S_2Te$: C, 55.81; H, 4.51; N, 3.95. Found: C, 55.67; H, 4.62; N, 3.82%. ^{1}H-NMR: δ 2.34s (6H, N–CH_3), 3.49s (2H, –CH_2–), 6.96m (3H, –C_6H_4–, H_{3-5}), 7.27m (12H, P–C_6H_5-*meta* + *para*), 7.65d (1H, –C_6H_4–, H_6, $^3J_{HH} = 7.2$ Hz), 7.83dd (4H, P–C_6H_5-*ortho*, $^3J_{HH} = 7.4$ Hz, $^3J_{PH} = 14.0$ Hz), 7.96 ddd (4H, P–C_6H_5-*ortho*, $^3J_{HH} = 6.9$ Hz, $^4J_{HH} = 2.2$ Hz, $^3J_{PH} = 12.9$ Hz). ^{31}P-NMR: δ 41.9s (P=S), 31.7s (P–S).

3.4. X-ray structure determination

Pale yellow, block crystals of $[2\text{-}(Me_2NCH_2)C_6H_4Te]_2$ (**1**), $[2\text{-}(Me_2NCH_2)C_6H_4]TeS(S)PMe_2$ (**2**), $[2\text{-}(Me_2NCH_2)C_6H_4]TeS(S)PPh_2$ (**4**), $[2\text{-}(Me_2NCH_2)C_6H_4]TeS(S)P(OPr^i)_2$ (**5**) and $[2\text{-}(Me_2NCH_2)C_6H_4]Te–S–PPh_2=N–PPh_2=S$ (**6**), were mounted on glass fibers. Data were collected on an Enraf Nonius KappaCCD area detector (φ scans and ω scans to fill Ewald sphere) at the University of Southampton EPSRC National Crystallography Service. Data collection and cell refinement [38] gave cell constants corresponding to an orthorhombic (for **1**), triclinic (for **4** and **5**) and monoclinic (for **2** and **6**) cells whose dimensions are given in Table 5 along with other experimental parameters.

An absorption correction was applied [39] which resulted in maximum and minimum transmissions ranging from 0.9426 to 0.5863 for **1**, 0.7651 and 0.8870 for **2**, 0.7786 and 0.8186 for **4**, 0.8438 and 0.7200 for **5**, and 0.9425 and 0.7148 for **6**. The absolute structure parameter for **6** was −0.057(14).

The structures were solved by direct methods [40]. All of the non-hydrogen atoms were treated anisotropically. The data for **4**, **5**, and **6** were of much better quality than those for **2**. The positions of the high residual peaks in the latter made no chemical sense but the similarity of the structures gives added confidence to the structure of **2** despite the relatively high *R* values. Hydrogen atoms were included in idealized positions with isotropic thermal parameters set at 1.2 times that of the carbon atom to which they were attached. The final cycle of full-matrix least-squares refinement [41] was based on 5337 for **1**, 2818 for **2**, 5293 for **4**, 4557 for **5** and 6003 for **6** observed reflections [3165 for **1**, 1938 for **2,** 4423 for **4,** 3950 for **5** and 5598 for **6**, for $F^2 > 2\sigma(F^2)$] and 203 for **1**, 149 for **2,** 237 for **4**, 200 for **5** and 363 for **6** variable parameters and converged (largest parameter shift was 0.001 times its e.s.d.).

4. Supplementary material

Crystallographic data for the structural analysis of compounds **1**, **2**, **4**–**6** have been deposited at The Cambridge Crystallographic Data Centre (CCDC nos. 148058 (**1**), 148059 (**2**), 148060 (**4**), 148061 (**5**), 148062 (**6**)). Copies of the information may be obtained free of

Table 5
X-ray crystal data and structure refinement for **1**, **2**, **4**–**6**

	1	**2**	**4**	**5**	**6**
Empirical formula	$C_{18}H_{24}N_2Te_2$	$C_{11}H_{18}NPS_2Te$	$C_{21}H_{22}NPS_2Te$	$C_{15}H_{26}O_2NPS_2Te$	$C_{33}H_{32}N_2P_2S_2Te$
Formula weight	523.59	386.95	511.09	475.06	710.27
Temperature (K)	150(2)	298(2)	298(2)	298(2)	150(2)
Wavelength (Å)	0.71073	0.71073	0.71073	0.71073	0.71073
Crystal system	Orthorhombic	Monoclinic	Triclinic	Triclinic	Monoclinic
Space group	*Pbca*	$P2_1/n$	$P\bar{1}$	$P\bar{1}$	$P2c$
Unit cell dimensions					
a (Å)	18.810(4)	15.414(3)	9.882(2)	10.122(2)	9.7420(19)
b (Å)	9.050(2)	5.6458(11)	10.424(2)	10.557(2)	9.1850(18)
c (Å)	22.926(5)	19.433(4)	12.318(3)	11.713(2)	17.672(4)
α (°)			66.11(3)	115.92(3)	
β (°)		103.90(3)	67.33(3)	106.33(3)	91.11(3)
γ (°)			84.36(3)	100.17(3)	
Volume (Å^3)	3902.7(15)	1641.7(6)	1068.0(4)	1013.2(3)	1581.0(5)
Z	8	4	2	2	2
D_{calc} (g cm^{-3})	1.782	1.566	1.589	1.557	1.492
Absorption coefficient (mm^{-1})	2.989	2.142	1.668	1.758	1.200
$F(000)$	2000	760	508	476	716
Crystal size (mm)	$0.20\times0.05\times0.02$	$0.25\times0.15\times0.07$	$0.30\times0.15\times0.15$	$0.20\times0.15\times0.10$	$0.30\times0.20\times0.05$
θ range for data collection (°)	3.07–30.45.	1.52–27.46	2.99–30.37	3.07–27.50	3.05 to 27.48.
Reflections collected	27143	7699	10468	11929	12601
Independent reflections	5337 [$R_{int}=0.0817$]	3555 [$R_{int}=0.0887$]	5293 [$R_{int}=0.0324$]	4557 [$R_{int}=0.0491$]	6003 [$R_{int}=0.0392$]
Maximum and minimum transmissions	0.9426 and 0.5863	0.7651 and 0.8870	0.7786 and 0.8186	0.8438 and 0.7200	0.9425 and 0.7148
Refinement method	Full-matrix least-squares in F^2	Full-matrix least-squares in F^2	Full-matrix least-squares in F^2	Full-matrix least-squares in F^2	Full-matrix least-squares in F^2
Data/restraints/parameters	5337/0/203	2818/0/149	5293/0/237	4557/0/200	6003/1/363
Goodness-of-fit on F^2	0.975	1.078	1.065	1.075	1.055
Final R indicies [$F^2>2\sigma(F^2)$]	$R_1=0.0441$, $wR_2=0.0725$	$R_1=0.1131$, $wR_2=0.3318$	$R_1=0.0351$, $wR_2=0.0788$	$R_1=0.0352$, $wR_2=0.0835$	$R_1=0.0310$ $wR_2=0.0729$
R indicies (all data)	$R_1=0.1069$, $wR_2=0.0882$	$R_1=0.1761$, $wR_2=0.3861$	$R_1=0.0461$, $wR_2=0.0850$	$R_1=0.0436$, $wR_2=0.0884$	$R_1=0.0358$ $wR_2=0.0759$
Largest difference peak and hole (e Å^{-3})	1.072 and −1.316	4.972 and −1.345	0.447 and −1.038	0.660 and −0.951	0.649 and −0.889

charge from The Director, CCDC, 12 Union Road, Cambridge CB2 1EZ, UK (Fax: +44-1223-336033; e-mail: deposit@ccdc.cam.ac.uk or www: http://www.ccdc.cam.ac.uk).

Acknowledgements

This work was supported by the Natural Sciences and Engineering Research Council of Canada and the Romanian National Council for High Education Scientific Research (CNCSIS).

References

[1] V.I. Minkin, I.D. Sadekov, A.A. Maksimenko, O.E. Kompan, Yu.T. Struchkov, J. Organomet. Chem. 402 (1991) 331.
[2] N. Sudha, H.B. Singh, Coord. Chem. Rev. 135/136 (1994) 469.
[3] T.A. Hamor, A.G. Maslakov, W.R. McWhinnie, Acta Crystallogr. Sect. C 51 (1995) 2062.
[4] R. Kaur, H.B. Singh, R.T. Butcher, Organometallics 14 (1995) 4755.
[5] M.R. Detty, A.J. Williams, J.M. Hewitt, M. McMillan, Organometallics 14 (1995) 5258.
[6] T.A. Hamor, H. Chen, W.R. McWhinnie, S.L.W. McWhinnie, Z. Majeed, J. Organomet. Chem. 523 (1996) 53.
[7] Z. Majeed, W.R. McWhinnie, T.A. Hamor, J. Organomet. Chem. 549 (1997) 257.
[8] H.B. Singh, N. Sudha, A.A. West, T.A. Hamor, J. Chem. Soc. Dalton Trans. (1990) 907.
[9] H.B. Singh, N. Sudha, R.T. Butcher, Inorg. Chem. 31 (1992) 1431.
[10] A.G. Maslakov, W.R. McWhinnie, M.C. Perry, N. Shaikh, S.L.W. McWhinnie, T.A. Hamor, J. Chem. Soc. Dalton Trans. (1993) 619.
[11] M.R. Detty, A.E. Friedman, M. McMillan, Organometallics 13 (1994) 3338.
[12] M.A.K. Ahmed, A.E. McCarthy, W.R. McWhinnie, F.J. Berry, J. Chem. Soc. Dalton Trans. (1986) 771.
[13] N. Al-Salim, A.A. West, W.R. McWhinnie, T.A. Hamor, J. Chem. Soc. Dalton Trans. (1988) 2363.

[14] A.A. West, W.R. McWhinnie, T.A. Hamor, J. Organomet. Chem. 356 (1988) 159.
[15] I. Haiduc, R.B. King, M.G. Newton, Chem. Rev. 94 (1994) 301.
[16] M.G. Newton, R.B. King, I. Haiduc, A. Silvestru, Inorg. Chem. 32 (1993) 3795.
[17] A. Silvestru, I. Haiduc, K.H. Ebert, H.J. Breunig, Inorg. Chem. 33 (1994) 1253.
[18] A. Silvestru, I. Haiduc, K.H. Ebert, H.J. Breunig, D.B. Sowerby, J. Organomet. Chem. 482 (1994) 253.
[19] A. Silvestru, I. Haiduc, H.J. Breunig, K.H. Ebert, Polyhedron 14 (1995) 1175.
[20] A. Silvestru, R.A. Toscano, I. Haiduc, H.J. Breunig, Polyhedron 14 (1995) 2047.
[21] S. Bjoernevag, S. Husebye, K. Maartmann-Moe, Acta Chem. Scand. A36 (1982) 195.
[22] S. Husebye, K. Maartmann-Moe, O. Mikalsen, Acta Chem. Scand. 44 (1990) 802.
[23] J.E. Drake, A. Silvestru, J. Yang, I. Haiduc, Inorg. Chim. Acta 271 (1998) 75.
[24] J.E. Drake, R.J. Drake, A. Silvestru, J. Yang, Can. J. Chem. 77 (1999) 356.
[25] J. Novosad, S.V. Lindeman, J. Marek, J.D. Woollins, S. Husebye, Heteroatom Chem. 9 (1998) 615.
[26] J. Novosad, K.W Törnroos, M. Necas, A.M.Z. Slawin, J.D. Woollins, S. Husebye, Polyhedron 18 (1999) 2861.
[27] D.J. Birdsall, J. Novosad, A.M.Z. Slawin, J.D. Woollins, J. Chem. Soc. Dalton Trans. (2000) 435.
[28] E. Huheey, Inorganic Chemistry: Principles of Structure and Reactivity, Walter de Gruyter Verlag, Berlin, 1988, p. 278.
[29] P.G. Llabres, O. Dideberg, L. Dupont, Acta Crystallogr. Sect. B 28 (1972) 2438.
[30] M.R. Spirlet, G. Van den Bossche, O. Dideberg, L. Dupont, Acta Crystallogr. Sect. B 35 (1979) 1727.
[31] B. Krebs, G. Henkel, Z. Anorg. Allg. Chem. 475 (1981) 143.
[32] K.C. Molloy, M.F. Mahon, I. Haiduc, C. Silvestru, Polyhedron 14 (1995) 1169.
[33] W. Kuchen, A. Rohrbeck, Chem. Ber. 105 (1972) 132.
[34] W. Kuchen, K. Strolenberg, J. Metten, Chem. Ber. 96 (1963) 1733.
[35] W. Kuchen, H. Meyatepeck, Chem. Ber. 101 (1968) 3454.
[36] A.E. Lippman, J. Organomet. Chem. 31 (1966) 471.
[37] R. Rösler, C. Silvestru, I. Haiduc, F. Kayser, M. Gielen, B. Mahieu, Main Group Met. Chem. 16 (1993) 435.
[38] Z. Otwinowski, W. Minor, Denzo. In: C.W. Carter Jr., R.M. Sweet (Eds.), Methods in Enzymology, vol. 207, Macromolecular Crystallography, Part A, Academic Press, 1997, p. 307.
[39] SORTAV: R.H. Blessing, Acta Crystallogr. Sect. A 51 (1995) 33; R.H. Blessing, J. Appl. Crystallogr. 30 (1997) 421.
[40] G.M. Sheldrick, Acta Crystallogr. Sect. A 46 (1990) 467.
[41] G.M. Sheldrick, SHELXL97, University of Göttingen, Germany, 1997.